

# Considerations on the accretion of Uranus and Neptune by mutual collisions of planetary embryos in the vicinity of Jupiter and Saturn

M. Jakubík<sup>1</sup>, A. Morbidelli<sup>2</sup>, L. Neslušan<sup>1</sup>, and R. Brasser<sup>2</sup>

<sup>1</sup> Astronomical Institute, Slovak Academy of Science, 05960 Tatranská Lomnica, Slovakia  
e-mail: mjakubik@ta3.sk; ne@ta3.sk

<sup>2</sup> Département Cassiopée, University of Nice - Sophia Antipolis, CNRS, Observatoire de la Côte d'Azur; Nice, France  
e-mail: morby@oca.eu; brasser\_astro@yahoo.com

Received ????? ??, 2011; accepted ????? ??, ????

## ABSTRACT

**Context.** Modeling the formation of Uranus and Neptune is a long-lasting problem in planetary science. Due to the gas-drag, collisional damping, and resonant shepherding, the planetary embryos repel the planetesimals away from their reach and thus they stop growing. This problem persists independently of whether the accretion took place at the current locations of ice giants or closer to the Sun.

**Aims.** Instead of trying to push the runaway/oligarchic growth of planetary embryos up to 10–15 Earth masses, we envision the possibility that the planetesimal disk could generate a system of planetary embryos of only 1–3 Earth masses. Then we investigate whether these embryos could have collided with each other and grown enough to reach the masses of current Uranus and Neptune.

**Methods.** We perform several series of numerical simulations. The dynamics of a considered set of embryos is influenced by the presence of Jupiter and Saturn, assumed to be fully formed and in their mutual 2:3 resonance, and gravitational interactions with the disk of gas.

**Results.** Our results point to two major problems. First, there is typically a large difference in mass between the first and the second most massive planet. Second, the final planetary system typically has more than two planets, beside Jupiter and Saturn. Our simulations suggest that it is difficult to grow major planets without having, at the end, a crowded planetary system. The growth of a major planet from a system of embryos requires strong damping of eccentricities and inclinations from the disk of gas. But strong damping also favors embryos and planets to find a stable resonant configuration, so that systems with more surviving planets are found. In addition to these problems, it is necessary to assume that the surface density of the gas was several times higher than that of the minimum-mass solar nebula, in order to have substantial mutual accretion among embryos. However this contrasts with the common idea that Uranus and Neptune formed in a gas-starving disk, which is suggested by the relatively small amount of hydrogen and helium contained in the atmospheres of these planets.

**Conclusions.** None of our simulations successfully reproduced the structure of the outer Solar System. However, our work has the merit to point out non-trivial problems that cannot be ignored and have to be addressed in future work.

**Key words.** planetary systems – planets and satellites: formation – planets and satellites: individual: Uranus, Neptune – protoplanetary disks

## 1. Introduction

The accretion of Uranus and Neptune is a long-standing problem in planetary science. Safronov (1969) was the first to point out that the accretion of these two planets from a planetesimal disk at their current locations would have taken implausibly long timescales. This problem was confirmed by Levison & Stewart (2001) using modern numerical simulations. Goldreich et al. (2004a,b) claimed that the in-situ formation of Uranus and Neptune could have been possible in a planetesimal disk strongly dominated by collisional damping. This claim, however, is not correct because, as showed by Levison & Morbidelli (2007), planetary cores in a disk with strong collisional damping simply open gaps in the planetesimal distribution around their own orbits and stop accreting.

There is now a consolidated view that the giant planets were closer to each other in the past (probably all within 12 AU from the Sun) and that they moved to their current orbits after their formation (Fernández & Ip 1984; Malhotra 1993, 1995; Hahn & Malhotra 1999; Thommes et al. 1999; Tsiganis et al. 2005; Morbidelli et al. 2007; Batygin & Brown 2010). Thus, it

is no longer necessary to construct a model capable of explaining the formation of Uranus and Neptune at their current, remote locations.

Forming Uranus and Neptune within 12–15 AU from the Sun is in principle easier than forming them at 20–30 AU because the density of solid material was probably higher and the dynamical timescale (i.e. the orbital period) was shorter. However, forming 10–15 Earth mass ( $M_{\oplus}$ ) cores from a planetesimal disk turns out to be difficult at *any* location. In fact, Levison et al. (2010) showed that, when planetary embryos achieve a mass of 1–3  $M_{\oplus}$ , they tend to scatter the remaining planetesimals away rather than accreting them. With the help of gas-drag, collisional damping and resonant shepherding, the embryos repel the planetesimals away from their reach and thus they stop growing.

In this paper we explore another possible venue for the formation of Uranus and Neptune. Instead of trying to push the runaway/oligarchic growth of planetary embryos up to 10–15  $M_{\oplus}$ , we envision the possibility that the planetesimal disk could generate a system of planetary embryos of only 1–3  $M_{\oplus}$ ; then we

investigate with numerical simulations whether these embryos could have collided with each other because they converged at specific orbital radii where their radial migration in the gas-disk was stopped by the presence of Jupiter and Saturn.

More specifically, our scenario is based on the consideration that Jupiter and Saturn presumably got caught in their mutual 2:3 mean motion resonance (MMR), which prevented them from migrating further towards the Sun. Instead, after being trapped in the 2:3 MMR, Jupiter and Saturn either migrated outwards or stayed roughly at steady locations (Masset & Snellgrove 2001; Morbidelli & Crida 2007; Morbidelli et al. 2007; Pierens & Nelson 2008). To date, this is the only explanation we have for why our giant planets did not migrate permanently into the inner Solar System.

The presence of Jupiter and Saturn on orbits not migrating towards the Sun would have acted as an obstacle against the inward Type-I migration of the planetary embryos from the outer Solar System. More precisely, any planetary embryo migrating towards the Sun would have been, sooner or later, trapped and halted in a mean motion resonance with Saturn. Then, the accumulation of embryos in these resonances could in principle have boosted their mutual accretion. This paper aims at investigating this possibility with numerical simulations.

We are aware of the new result according to which the real migration of planetary embryos is very different from the classical Type-I migration envisioned in ideal, isothermal disks (Paardekooper & Mellema 2006; Baruteau & Masset 2008; Paardekooper & Papaloizou 2008; Kley & Crida 2008; Paardekooper et al. 2011). In particular, in disks with realistic cooling times, migration is expected to be outward in the inner part of the disk and inward in its outer part (Lyra et al. 2009). This generates a region in between the inner and the outer parts of the disk where Type-I migration is basically inhibited. Planetary embryos are expected to be in/close this no-migration zone, which seems to invalidate our assumption that embryos migrated towards the giant planets until they got captured in resonances.

However, Walsh et al. (2011), from constraints provided by the terrestrial planet system and the asteroid belt, argued strongly that Jupiter and Saturn migrated outwards over a range of several AUs. What is important for our purposes is the relative motion of Jupiter/Saturn and the embryos. It does not really matter whether Jupiter/Saturn are on fixed orbits and the embryos tend to migrate towards the Sun, or the embryos do not migrate while Jupiter/Saturn move outwards. In fact, in both cases the embryos approach the giant planets until they are captured in MMRs, which may act like a privileged site for embryo clustering and mutual accretion. Thus, in our simulations, for simplicity we assume that Jupiter/Saturn are on non-migrating resonant orbits while the embryos are affected by inward migration, with different migration speeds from one simulation to another. This migration speed can be interpreted as an actual inward migration speed of the embryos (most likely reduced relative to the classical Type-I migration speed in iso-thermal disks), or the outward migration speed of Jupiter/Saturn or a combination of the two.

Two caveats related to our work need to be stated up-front. First, our study assumes that Jupiter and Saturn are fully formed, while the accretion of these planets is by itself an unsolved problem that we don't address here. This may sound strange. However, there is a consensus that Uranus and Neptune formed after Jupiter and Saturn, because they did not accrete nearly as much of gas. This leads to two considerations: (a) Jupiter and Saturn existed already when Uranus and Neptune formed, so that the former should/may have influenced the accretion pro-

cess of the latter and (b) whatever mechanism allowed the formation of Jupiter (obviously not the presence of a pre-existing giant planet!), it did not work for Uranus and Neptune, otherwise they would have formed nearly at the same time as Jupiter.

The second caveat is that, because our model is based on migration of planets and embryos in a gas-disk, the study should be performed with hydro-dynamical simulations. These simulations, though, are too slow to treat the evolution of tens of bodies for a few millions of years, as we need to perform in this study. The paper by Morbidelli et al. (2008) is, to date, the only attempt to study the accretion of the cores of giant planets using hydro-dynamical simulations, and it shows all the limitations of this technique. Thus, for this study we use N-body simulations, with artificial forces exerted onto the embryos to mimic the migration and tidal damping forces exerted from the disk. This approach also has its own limitations as it does not account for indirect mutual perturbations that the embryos may exert onto each other through the modifications that they induce in the density distribution of the gas-disk.

The structure of this paper is as follows. In Sect. 2, we explain our simulation methods. In Sect. 3 we illustrate some basic ingredients of the dynamics of embryos and giant planets. In particular, we discuss the concept of resonance trapping with Saturn, resonant trapping in mutual embryo-embryo resonances, resonance loading, onset of a global dynamical instability and possible mutual accretion. Just for illustrative purposes, we do this by introducing one embryo at the time at a large distance from Saturn, even though this is NOT how we think the real evolution proceeded. Then, in Sect. 4 we move to more “realistic” simulations, where multiple  $3 M_{\oplus}$  embryos are introduced at the beginning of the simulation over the 10–35 AU range. We test the dependence of the results on the total amount of gas in the disk, the inward migration rate and the total number of embryos. Having realized that several embryos are lost by having close encounters with Jupiter and Saturn which either eject them onto distant orbits or inject them into the inner Solar System, in Sect. 5 we show how the coorbital corotation torque exerted at the edge of Saturn's gap can act like a planet trap (Masset et al. 2006; Pierens & Nelson 2008) and prevent mass loss. In Sect. 6 we discuss how the results depend on the initial mass of the embryos. In Sect. 7 we address the role of turbulence in the disk and Sect. 8 collects the conclusions and considerations that we derive from this study.

We anticipate that our study is not “successful”, in the sense that our simulations do not typically lead to the formation of only two planets with masses close to those of Uranus and Neptune. However it shows interesting dynamical mechanisms and intriguing consequences that will need to be addressed in detail in future studies, most likely using hydro-dynamical simulations.

## 2. Simulation Methods

For our simulations, we use the integration software *Symba* developed in Duncan et al. (1998), that we modified in order to take into account the planet-gas gravitational interactions.

The gas density profile that we consider is taken from the hydro-dynamical simulations of Morbidelli & Crida (2007), which accounted for Jupiter and Saturn in their mutual 2:3 resonance; it is shown in Fig. 1 (red curve). Notice the gap opened around the position of Jupiter at 5.2 AU and the “plateau” at the right hand-side of the gap, which is due to the presence of Saturn at  $\sim 7$  AU. The figure also compares this density profile to those of three classical *Minimal Mass Solar Nebulae* (MMSN). In the 10–35 AU range, the surface densities are comparable, within an

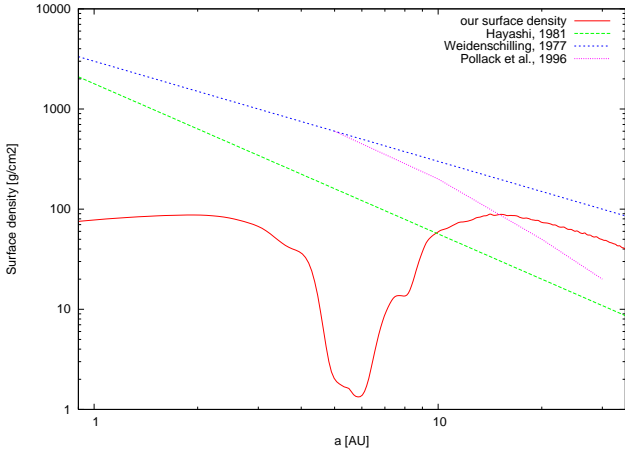


**Fig. 1.** Gas surface densities according to different works. The red curve shows the result of a hydro-dynamical simulation by Morbidelli & Crida (2007), with Jupiter and Saturn in the mutual 2:3 resonance. This is the profile that we assume in this paper, possibly scaled by a factor  $f_d$ . The blue line is from Weidenschilling (1977) and is proportional to  $1/r$ . The green line from Hayashi (1981) and is proportional to  $1/r^{3/2}$ . The magenta curve reports the amount of gas required in Pollack et al. (1996) model of giant planet accretion.

order of magnitude. In particular, our surface density falls in between the estimates from Weidenschilling (1977) and Hayashi (1981). Instead, inside of the orbit of Jupiter, the radial profile of our surface density is flat and significantly lower than those expected from the authors above. This is because the presence of Jupiter opens a partial cavity inside its orbit, by limiting the flow of gas from the outer part of the disk (see Crida et al. 2007). In Morbidelli & Crida (2007) the considered disk was narrow, with an outer boundary at 35 AU. Here, we extend its surface density profile beyond 35 AU assuming a  $r^{-3/2}$  radial decay.

The concept of MMSN was historically introduced assuming that giant planet formation was 100% efficient. In reality, there is growing evidence that much more mass is needed to grow the giant planets, even in the most optimistic scenarios (Thommes et al. 2003). Therefore, in our simulations we multiply the assumed initial surface density profile by a factor  $f_d$ , which will be specified from simulation to simulation. Moreover, at each time step  $dt$  the surface density is multiplied by a factor  $(1 - dt/\tau)$ , so that the density at any point in space decays as  $\exp(-t/\tau)$ . Unless otherwise specified, we assume that  $\tau = \infty$  during the first 5 My (so that there is no time-decay of the disk’s surface density over this period), then we assume  $\tau = 0.5$  My, i.e. a fast time-decay. This is in agreement with observational and theoretical results arguing that the photo-evaporation of disks starts after several millions of years, but then proceeds very quickly (Alexander et al. 2006a,b).

In our code, the surface density profile of the gas is used to compute the migration and damping forces acting onto the embryos, namely the so-called “type-I torques”. The analytic formulae that we use are those reported in Cresswell & Nelson (2008); they depend on the local surface density of the disk and on the embryos’ eccentricities and inclinations. Because inward migration can be significantly slower in realistic disks with radiative transfer than in ideal, isothermal disks, we give ourselves the possibility of multiplying the forces acting on the embryo’s semi major axes by a factor  $1/f_i$ , which will be specified below for each simulation.

However, in Sect. 5, we use a more sophisticated formula for the radial migration torque  $\Gamma$ , which accounts for the radial gradient of the surface density (Paardekooper et al. 2010; Lyra et al. 2010):

$$\Gamma = \Gamma_0(-0.85 - \alpha - 0.9\beta), \quad (1)$$

where  $\Gamma_0 = (M/h)^2 \Sigma r^4 \Omega^2$ ,  $M$  is the mass of the embryo relative to the Sun,  $h$  is the scale-height of the disk,  $\Sigma$  stands for the local surface density, and  $\Omega$  is the orbital frequency. In (1)

$$\alpha = -\frac{d \log \Sigma}{d \log r}, \quad \beta = -\frac{d \log T}{d \log r}, \quad (2)$$

where  $T$  is the local temperature of gas.

The radial migration torque in Cresswell & Nelson (2008), at zero order in eccentricity and inclination, corresponds to (1) for  $\beta = 1$  and  $\alpha = 0$ , i.e. it is valid for a flat disk with constant scale height. The inclusion of the  $\alpha$ -dependence in (1) stops inward migration where  $\alpha = -1.75$ , that is where there is a steep positive radial gradient of the surface density. With the surface density profile shown in Fig. 1, this happens at  $\sim 10$  AU. This location acts like a planet trap (Masset et al. 2006): an embryo migrating inwards from the outer disk, if not trapped in a mean motion resonance with Saturn, is ultimately trapped at this location.

In the simulations that mimic turbulent disks (see Sect. 7), we simply apply stochastic torques to the embryos following the recipe extensively described in Ogihara et al. (2007); see Sect. 2.2 of that paper). The only difference is that the total number of Fourier modes in the torque spectrum is not  $m = 50$ , as in Ogihara et al. (2007), but is  $m = 50 / \log 4 \times \log(r_{\text{out}}/r_{\text{in}})$  which, given  $r_{\text{out}} = 24$  AU and  $r_{\text{in}} = 8$  AU in our case, makes  $m = 40$ . This functional form for  $m(r_{\text{out}}, r_{\text{in}})$  is necessary in order to make the results independent of the simulated size of the disk. In fact, if one used a fixed number of Fourier modes, the effect of turbulence would be stronger in a narrow disk than in an extended disk. With our recipe for the number of modes, the stochastic migration of planetesimals observed in the full MRI simulations of Nelson & Gressel (2010) is reproduced with a “turbulent strength” parameter  $\gamma$  (see eq. 6 in Ogihara et al. (2007)) equal to  $3 \times 10^{-3}$ .

A final technical note concerns the treatment that we reserve to Jupiter and Saturn. The migration of these two planets is a two-planet Type-II-like process (Masset & Snellgrove 2001; Morbidelli & Crida 2007), and therefore cannot be described with the Type-I torques reported above. As stated in the Introduction, we assume that the disk parameters are such that Jupiter and Saturn do not migrate (see Morbidelli & Crida (2007), for the identification of the required conditions). Consequently, one could think that we should apply no fictitious forces to these planets. However, if we did so, the system would become unstable. In fact, as soon as an embryo is trapped in a resonance with Saturn, it would push Saturn inwards and in turn also Jupiter (because Jupiter and Saturn are locked in resonance). This would also increase the orbital eccentricities of the two major planets. This behavior is obviously artificial, because we do not consider the forces exerted by the gas onto Jupiter and Saturn, which would stabilize these planets against the perturbations from the much smaller embryo. To circumvent this problem, we apply damping forces to Jupiter and Saturn so that  $de/e = di/i = 10^{-5}/y$ , together with a torque that tends to restore the initial semi major axes of their orbits in  $10^5$  years. Tests show that, with this recipe, Jupiter and Saturn are stable under the effect of embryos piling up in resonances and pushing inwards.

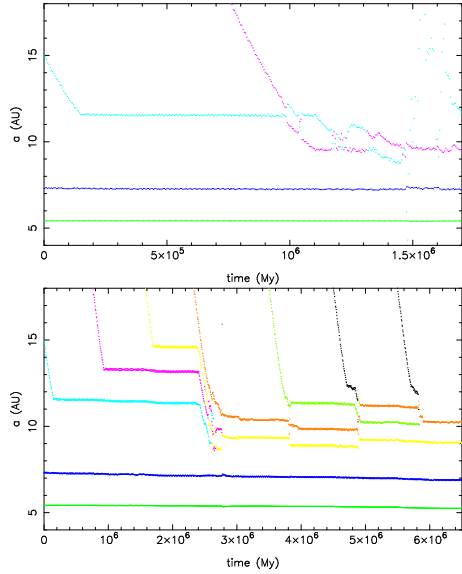


**Fig. 2.** Simulations of the dynamical evolution of embryos in the disk outside of Saturn’s orbit. Top: a case with parameters  $f_d = f_l = 1$ . Bottom, a case with  $f_d = f_l = 2$ . The green and blue curves at  $\sim 5.4$  and  $\sim 7.3$  AU show the semi major axis evolution of Jupiter and Saturn, respectively. The other curves of various colors illustrate the evolution of the semi major axes of the embryos. See text for a description of the dynamical evolution and the accretion events.

Moreover the eccentricities of Jupiter and Saturn attain finite but non-zero limit values.

In the final part of the simulation ( $t > 5$  My) when the surface density of the gas is reduced by a factor  $\exp[(t - 5)/\tau]$ , we also reduce the damping and restoring torques that act on Jupiter and Saturn by the same amount. This is necessary to avoid an artificial secular change of the orbits of the giant planets during the gas-dissipation phase.

### 3. Basic dynamical mechanisms in mutual migration of embryos and giant planets

To illustrate the interplay between migration, resonance trapping and mutual scattering, in this section we do simple experiments, where we introduce in the system one embryo at the time. The time-span between the introduction of two successive embryos is not fixed: we let the system relax to a stable configuration before introducing a new embryo in the simulation. Each embryo has initially  $3 M_\oplus$ .

We start by assuming the nominal values of the parameters ( $f_d = 1$ ,  $f_l = 1$ ). The top panel of Fig. 2 shows the evolution. The first embryo is introduced at the beginning of the simulation at 15 AU. It migrates inwards (cyan dotted curve) until it is trapped in resonance with Saturn (precisely the 1:2 MMR) at  $t \sim 150,000$  y. Thus, it stops migrating. Resonance trapping converts the force acting onto the semi major axis into an eccentricity excitation. Thus, the eccentricity of the embryo grows to about 0.07 but then it stops (not shown in figure). This happens because a balance is reached between the eccentricity excitation from the resonance and the direct damping from the disk. Thus, the three-planet system (Jupiter, Saturn and the embryo) reaches a stable, invariant configuration at about  $t = 200,000$  y.

At  $t = 750,000$  y we introduce a second embryo in the system, initially at 18 AU. This embryo also migrates inward (ma-

genta dotted line). It is not trapped in any MMR, so that it comes down to  $\sim 12$  AU and starts to have close encounters with the cyan embryo. The system becomes unstable. The eccentricities and inclinations of the embryos become very large, up to 0.6–0.7 and 10 degrees respectively. The cyan embryo has even close encounters with Saturn and Jupiter. It is clear that this phase of violent scattering is not very favorable for embryo-embryo accretion.

We then present another simulation, where we increase the gas surface density by a factor of two ( $f_d = 2$ ), which has the effect of increasing both the eccentricity/inclination damping and the radial migration by the same factor. However, we also assume  $f_l = 2$ , so that the migration rate of the semi major axis is in fact the same as in the previous simulation. The result of this new simulation is illustrated in the bottom panel of Fig. 2. As one can see, the magenta embryo is now trapped in resonance with the cyan embryo (precisely, the 4:5 MMR). So, it also stops migrating and a stable four-planet configuration is achieved. Given that the only difference with respect to the previous simulation is the eccentricity damping, this illustrates the crucial role of this parameter on the dynamics.

A third embryo (yellow) is introduced at  $t = 1.6$  My. It also migrates until it stops, trapped in the 6:7 MMR with the cyan embryo. The fully resonant system is, again, stable.

A fourth embryo is then released at  $t = 2.3$  My (orange). Now there are too many embryos to form a stable, resonant system. So, when the orange embryo comes in, resonance locking is broken. All embryos move inward and start to have encounters with each other. Because of the stronger damping from the disk, the eccentricities and inclinations do not become as large as in the previous experiment. Thus, the conditions are more favorable for mutual accretion. In fact, at  $t = 2.64$  My the yellow and cyan embryos accrete each other. Arbitrarily, we assume that it is the yellow embryo that survives, with twice its original mass and the cyan embryo disappears. The system of embryos, however, is still too excited to be stable. It stabilizes only after the ejection of the magenta embryo at  $t = 2.9$  My. The system is now made of two embryos, the yellow and orange ones, in their mutual 6:7 MMR. The yellow embryo is in the 2:3 MMR with Saturn.

We proceed the experiment by introducing a new embryo (green) which, after a short phase of instability, ends in the 4:5 MMR with the orange embryo and forces the orange and yellow embryos to go to smaller heliocentric distances: the yellow embryo ends in the 5:7 MMR with Saturn. Given the high-order resonances involved, the system is close to an instability.

Thus, when the next embryo (black) is introduced and moves inwards, the system becomes unstable. The new crisis is solved with the yellow embryo accreting the black one. At the end of the instability phase, the yellow embryo is back into the 2:3 MMR with Saturn and the three surviving embryos are in resonance with each other.

The final embryo is introduced at 5.5 My (black again). Given the illustrative purpose of this experiment, we keep  $\tau = \infty$  also beyond 5 My, so that the surface density of the gas does not evolve. The new embryo generates a new phase of instability during which it first collides with the orange embryo, then the orange embryo accretes also the green one. Therefore, this simulation ends with two embryos, each with a mass of  $9 M_\oplus$ , in a stable resonant configuration: the yellow embryo is in the 2:3 MMR with Saturn and in the 6:5 MMR with the orange one.

These experiments, as well as other similar ones that we do not present for brevity (with  $f_d = f_l = 3, 5$  and  $f_d = 1, f_l = 3$ ), show well the importance of mutual resonances in the evolution of the embryos. For individual masses equal to  $3 M_\oplus$ , embryos

are easily trapped in mutual resonances if  $f_I \geq 2$ . If the embryos are smaller,  $f_I$  needs to be larger, because the mutual resonant torques are weaker. A system of several embryos, all in resonance with each other, can be stable; if this is the case, mutual accretion is not possible. However, when the embryos are too numerous, resonances cannot continue to hold the embryos on orbits well separated from each other. The system eventually has to become unstable; collisions or ejections then occur. Finally, when the number of embryos is reduced, a new, stable resonant configuration is achieved again. This sequence of events (resonance loading, global dynamical instability, accretion or ejection) can repeat cyclically, as long as mass is added to the system. Eccentricity and inclination damping from the disk also plays a pivotal role in the evolution of the system. If damping is weak, eccentricities and inclinations can become large and scattering dominates over mutual accretion; eventually embryos encounter Jupiter or Saturn and are ejected from the system. If damping is large, the most likely end-state of a dynamical instability is the mutual accretion of embryos, which leads to the growth of massive planets.

Of course, the experiments presented in this section are not realistic, as embryos are introduced one by one. They are just intended to illustrate the basic dynamical mechanisms at play. In the next section, we present more realistic simulations, with all embryos simultaneously present from  $t = 0$ .

#### 4. A first attempt to form Uranus and Neptune

We present a series of simulations with 14 embryos originally distributed in semi-major axis from 10 to 35 AU. The initial orbits have low eccentricities ( $e \sim 10^{-2}$ ) and inclinations ( $i \sim 10^{-2}$  rad) relative to the common invariable plane of the system. The initial mass of each embryo is assumed to be  $3 M_\oplus$  and the mutual orbital separation among embryos is 5 Hill radii. We run simulations with  $f_d = 1, 2, 3$ , and 4, which progressively increase the effects of eccentricity/inclination damping. As well, we divide the speed of Type-I migration, by the factor  $f_I = 1, 4$  or 10. Every simulation is run for 8 My. After this period, the gas is practically gone and surviving embryos move on quasi-stable orbits.

The results of these simulations are summarized in Table 1. In the environment with the standard magnitude of gas density (i.e.  $f_d = 1$ ) there are no merging events leading to relatively massive embryos on quasi-stable orbits. The masses of almost all embryos surviving at the end of the simulations have not increased above the initial value. Merging events forming more massive objects occur in a denser environments, with  $f_d = 2$  and 3. Unfortunately, the simulations (with the exception of the first one labelled A12) do not produce more than one body with a final mass of 12 to  $15 M_\oplus$ , comparable to the current mass of Uranus or Neptune. The masses of the other surviving embryos remain equal to the initial value or grow insufficiently.

In few simulations, one or two large embryos, with a mass comparable to that of Uranus or Neptune, are formed, but they are lost before the end of simulation. For example, embryos with masses 12 and  $6 M_\oplus$  are formed in sim. A3 (see values of  $m_{max}$  in Table 1), none of these two objects survives at 8 My.

In all simulations, a large fraction of the initial mass in embryos ( $42 M_\oplus$ ) is lost. Embryos are accreted by Jupiter and Saturn, moved to the interior of Jupiter’s orbit, or ejected from the system. At the end, the total mass of survivors typically varies from 6 to  $27 M_\oplus$ . Only in a single simulation, A12, the entire initial mass of  $42 M_\oplus$  is conserved, although not all of

**Table 1.** Summary of the simulations starting with 14 planetary embryos. In addition to  $f_d$  and  $f_I$ , the table reports the three largest masses,  $m_{max}$ , ever achieved during the simulation, and the masses,  $m_{fin}$ , and semi-major axes,  $a_{fin}$ , of the embryos surviving at the end of simulation.

No.	$f_d$	$f_I$	$m_{max}$	$m_{fin}$	$a_{fin}$
A1	1	1	3, -, -	3, 3	9.6, 165
A2	1	4	6, 3, -	7×3	0.82, 1.1, 1.5 9.5, 11.5, 11.5, 13.3
A3	1	10	12, 6, 3	3, 3, 3	10.9, 12.4, 14.0
A4	2	1	6, 3, -	6, 3, 3	9.9, 9.9, 189
A5	2	4	12, 6, 3	3, 12, 6, 3	0.63, 9.9, 9.9, 12.5
A6	2	10	9, 3, -	3, 9, 3	0.82, 10.0, 13.1
A7	3	1	15, 6, 3	15, 6	0.30, 9.1
A8	3	4	15, 6, 3	15, 6, 3	0.22, 9.9, 11.3
A9	3	10	6, 3, -	3, 6, 6, 6, 3	0.63, 9.4, 9.4, 10.5, 11.4
A10	4	1	18, 6, 3	6	0.63
A11	4	4	9, 6, 3	6, 3, 9, 6	0.56, 1.2, 9.0, 10.4
A12	4	10	18, 12, 6	6, 18, 12, 3, 3	0.63, 8.4, 9.8, 11.4, 12.5

it is beyond Saturn. Notice that the injection of embryos inside the orbit of Jupiter (which happens in most simulations, see Table 1) is probably inconsistent with the current structure of the Solar System, but might explain the structure of some extra-solar planetary systems, particularly those with a hot Neptune and a more distant giant planet like HD 215497. Similarly, the ejection of embryos onto distant, long-period orbits (see  $a_{fin}$  in sims. Nos. A1 and A4) might find one day an analog in the extra-solar planet catalogues.

The simulations with  $f_d = 1$  result, on average, in smaller final embryos than those with  $f_d = 2$  and the latter result in smaller final masses than those with  $f_d = 3$ . However, this increase in the final masses does not continue for  $f_d = 4$ . Similarly, the simulations with  $f_I = 1$  and 4 suggest a broad correlation between the total final mass and the reduction factor for Type-I migration. Again, this trend does not continue in simulations with  $f_I = 10$ . The simulations with  $f_I = 1$  and 4 also suggest a correlation between the number of surviving embryos and  $f_I$ . In fact, while the average number of surviving embryos is 2 for  $f_I = 1$ , it becomes 4–5 for  $f_I = 4$ . But the final number of bodies remains  $\sim 4$  if the reduction factor  $f_I = 10$  is applied.

The large number of surviving embryos per simulation is at odds with the current structure of the outer Solar System, which has only Uranus and Neptune beside Jupiter and Saturn. In principle, some rogue embryos could have been eliminated during the dynamical instability that characterizes the late evolution of the outer Solar System in the so-called “Nice model” (Gomes et al. 2005), but this has never been demonstrated. In our accretion simulations, the existence of multiple embryos is a generic outcome, and is related to the fact that resonances can easily stabilize a system with more than two embryos, as shown in the previous section. Among the resonant configurations in which our final embryos are locked into, the 1:1 resonance is not uncommon (see sims. A2, A4, A5, or A9).

Let us now discuss some specific simulations. The standard initial conditions are assumed in simulation A1, with  $f_d = f_I = 1$ . The dynamical evolution of bodies in this simulation is shown in Fig. 3. We can see a very chaotic evolution of the system in



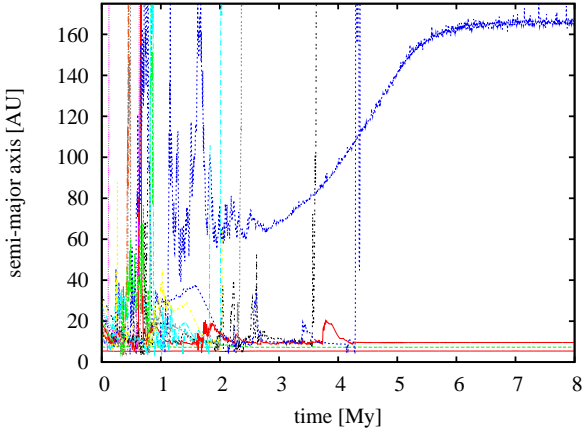


**Fig. 3.** The evolution semi-major axes of bodies in simulation A1 (see Table 1).

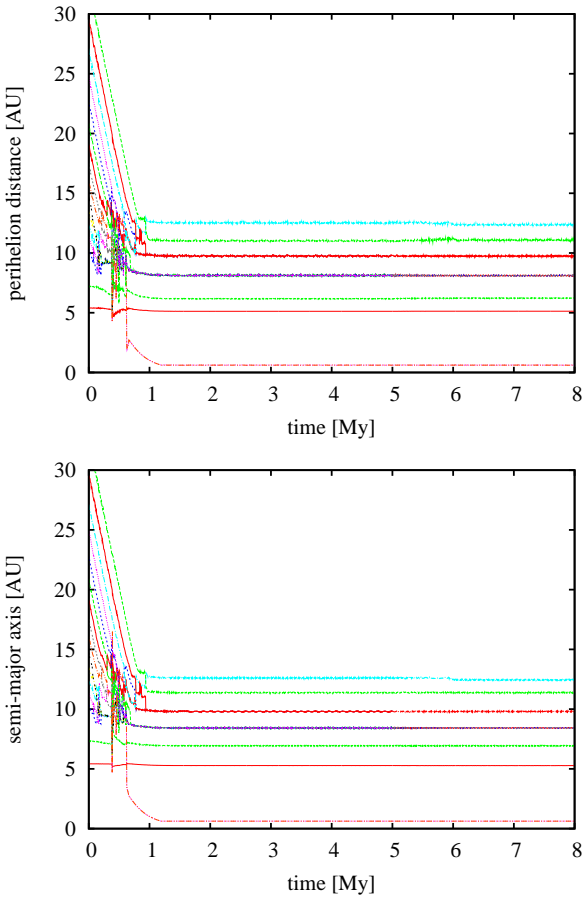


**Fig. 4.** The evolution of perihelion distance (upper plot) and semi-major axis (down plot) of bodies in simulation A12 (see Table 1).

an early era, characterized by migration and close encounters, which is typical of all our simulations. Here this chaotic phase is protracted for 4 Myr. No single merging event happens. A total of 12 embryos are ejected from the system. Two remain in the end, one of which on an orbit with  $a = 165$  AU. Obviously, in this simulation the damping is too low and type-I migration too strong. This is consistent with what we illustrated in Sect. 3.

In sims. A5, A6, A11, and A12, one (two in A12) embryo with the mass equal or larger than  $9 M_{\oplus}$  survives beyond Saturn (see Table 1). In sim. A5, this embryo, with a mass of  $12 M_{\oplus}$ , is in a horseshoe orbit with another embryo of  $6 M_{\oplus}$ . There are two redundant  $3 M_{\oplus}$  embryos, the first beyond the two more massive ones and the second interior to Jupiter’s orbit. Sim. A6, has, again, a  $3 M_{\oplus}$  embryo interior of Jupiter; the  $3 M_{\oplus}$  formed beyond Saturn is accompanied by a second embryo in an outer mean motion resonance, preserving its initial mass. Two relative massive surviving embryos ( $9$  and  $6 M_{\oplus}$ ) beyond Saturn are the result of sim. A11. However, also two embryos in terrestrial-planet-type orbits survive, one of them quite massive ( $6 M_{\oplus}$ ).

Two embryos beyond Saturn with masses  $18$  and  $12 M_{\oplus}$ , which are comparable to the current Uranus and Neptune, occur only in sim. A12. The evolution of semi-major axes of bodies in this simulation is shown in Fig. 4. Unfortunately, few problems occur also in this simulation. A massive,  $6 M_{\oplus}$  embryo reaches a  $0.63$  AU orbit and another two redundant embryos survive at the end in the outer region. This simulation is interesting because all the initial mass survives in the full  $8$  My simulation. However, the resulting system is too compact and becomes unstable in a continuation of the simulation beyond this time.

One could think that our inability to produce objects as massive as Uranus and Neptune is due to an insufficient total mass in embryos in the disk beyond Saturn. To investigate if this is true, we performed another series of simulations with more embryos and, therefore, a higher initial total mass. Specifically, we consider  $26$  or  $37$  embryos distributed in the range of heliocentric distances from  $8$  to  $33$  AU. The initial mass of each embryo is assumed to be  $3 M_{\oplus}$ , again. With this set-up, the orbital separation between embryos is on average smaller than  $5$  Hill radii. So, the embryos are on orbits which are closer to each other than predicted by the theory of runaway/oligarchic growth. We nevertheless assume such initial configurations in order to explore the dependence of the results on the total initial mass.

The masses and semi major axes of the surviving objects in this series of simulations after  $8$  Myr (a short time after the gas is gone), are given in Table 2, PART A. These states can be compared to those given in Table 1. Despite having more mass, on average we do not get more massive objects beyond Saturn. Increasing the initial mass, we basically just increase the mass loss. Notice that here we consider also the embryos injected inside Jupiter’s orbit as “lost planets”. In fact, the new set of simulations produce more numerous and more massive planets injected into the inner Solar System. Several “hot Neptunes” or super-Earths are formed.

Moreover, as in the initial series of runs, there are in general too many surviving planets beyond Saturn. Several cases of embryos moving in horseshoe orbits are observed.

Despite most simulations not providing good results, Sims. B7, B8 and, to a lesser extent, B8b, look encouraging. In these simulations at  $8$  Myr, there is one embryo with mass  $\geq 12 M_{\oplus}$  and another with mass  $\geq 9 M_{\oplus}$  beyond the orbit of Saturn. In sim. B8, the most massive embryos in this region have masses  $18$  and  $15 M_{\oplus}$ , which mimic the masses of Uranus and Neptune exceptionally well. These simulations are characterized by parameters  $f_d = 2$  and  $f_l = 4, 10$  respectively, which stresses the importance of enhancing damping and reducing migration speed to achieve significant accretion. On the other hand, in addition to the main “major” planets described above, there are several surviving embryos in all these relatively “successful” simulations. As in the previous series of runs, a large value of  $f_l$  appears to favor a larger number of surviving embryos. This is not surprising: when the embryos are forced to migrate faster (i.e. small

**Table 2.** The same as Table I, but for the simulations starting with more than 14 embryos. Here, the second column reports the number  $N$  of initial embryos.

No.	$N$	$f_d$	$f_I$	$m_{max}$	$m_{fin}$	$a_{fin}$
PART A – in 8 My						
B1	26	1	1	6, 3, -	4×3	9.5, 9.6, 35.0, 58.1
B1b	25	1	1	6, 3, -	3, 3	0.63, 27.8
B2	26	1	2	9, 6, 3	3, 9, 3, 3, 6, 3, 3	0.82, 9.5, 11.1, 11.1, 12.4, 13.8, 15.1
B3	26	1	4	6, 3, -	5×3	0.82, 11.7, 13.6, 17.4, 19.7
B4	26	1	10	12, 6, 3	3, 12, 3, 3, 6, 6, 4×3	2.2, 10.2, 12.8, 13.7, 16.3, 18.4, 20.8, 23.0, 25.3, 27.8
					10×3	17.8, 19.8, 21.6, 24.3, 27.5, 30.2, 33.9
B5	26	2	1	9, 3, -	9, 3, 3	0.33, 8.8, 10.0
B6	26	2	2	15, 6, 3	15, 6, 3	0.33, 9.5, 11.1
B7	26	2	4	15, 9, 6	3, 15, 6, 6, 9, 3	2.2, 9.5, 9.5, 11.6, 13.1, 14.8
B8	26	2	10	18, 15, 6	18, 15, 6×3	9.9, 12.1, 13.6, 15.1, 16.2, 18.3, 20.1, 21.7
B8b	25	2	10	12, 6, 3	3, 12, 12, 6, 4×3	2.8, 9.5, 11.6, 14.0, 15.6, 17.2, 18.9, 20.9
B9	26	3	1	18, 9, 6	6, 3, 6	0.63, 9.5, 9.5
B10	26	3	2	21, 6, 3	21, 3	0.30, 13.6; (J+S)
B11	26	3	4	15, 12, 6	12, 15, 6, 6	0.63, 8.8, 10.3, 11.7
B12b	25	3	10	15, 12, 6	15, 12, 5×3	9.2, 12.1, 13.9, 14.9, 16.2, 17.7, 20.8
B13	26	4	1	27, 6, 3	27, 6, 3, 3	0.22, 9.8, 9.8, 10.9
B14	26	4	2	24, 6, 3	24, 3, 3	0.22, 1.0, 10.1
B15	26	4	4	15, 9, 6	9, 6, 6, 3, 3	0.12, 9.9, 10.0, 11.1, 12.1
B16	26	4	10	12, 9, 6	3, 3, 12, 9, 6, 6, 5×3	0.82, 8.6, 8.6, 10.0, 10.9, 12.1, 13.5, 13.5, 14.4, 15.7, 17.1; (J+S)
B17	37	1	10	9, 6, 3	6, 3, 3, 9, 9, 6, 3, 6, 9×3	0.82, 2.2, 2.6, 9.8, 11.6, 14.0, 14.0, 16.2, 18.4, 20.1, 22.0, 24.7, 28.1, 30.9, 34.5, 38.0, 41.7
B18	37	2	10	9, 6, 3	9, 3, 9, 6, 6, 3, 6, 6, 4×3	0.82, 1.7, 10.0, 11.6, 13.0, 15.1, 15.2, 17.8, 19.4, 21.4, 23.5, 26.1
B19	37	3	10	12, 9, 6	3, 3, 6, 12, 9, 6, 4×3	0.82, 10.7, 10.7, 10.7, 12.4, 14.0, 16.3, 16.3, 17.8, 19.7
B20	37	4	10	36, 15, 6	36, 3, 3×6, 3, 6	0.33, 9.9, 12.0, 13.4, 14.6, 16.2, 17.8
PART B – in 50 My						
B1	26	1	1	6, 3, -	4×3	9.5, 9.6, 16.4, 47.8
B2	26	1	2	12, 6, 3	3, 12, 3	0.82, 11.7, 14.2
B3	26	1	4	6, 3, -	5×3	0.82, 11.7, 13.8, 17.5, 19.7
B4	26	1	10	12, 6, 3	3, 12, 3, 6, 6, 3, 3, 6	1.8, 10.5, 12.5, 15.1, 17.5, 22.1, 22.4, 28.2
B5	26	2	1	9, 6, 3	9, 6	0.33, 9.3
B6	26	2	2	15, 6, 3	15, 6, 3	0.33, 9.6, 11.1
B7	26	2	4	15, 9, 6	3, 15, 6, 9, 6, 3	1.1, 9.9, 9.9, 12.2, 13.9, 16.3
B8	26	2	10	21, 15, 6	15, 6	15.5, 31.7
B9	26	3	1	18, 9, 6	6, 6, 3	0.63, 9.9, 9.9
B10	26	3	2	21, 6, 3	21, 3	0.30, 13.6; (J+S)
B11	26	3	4	15, 12, 6	12, 15, 6, 6	0.63, 9.1, 10.5, 12.5
B13	26	4	1	27, 6, 3	27, 6	0.21, 11.4
B14	26	4	2	24, 6, 3	24, 3, 3	0.22, 1.0, 10.2
B15	26	4	4	15, 9, 6	9, 6, 6, 3, 3	0.12, 10.0, 10.0, 11.1, 12.1
B16	26	4	10	21, 9, 6	3, 21, 9, 6, 3×3	0.82, 8.5, 10.0, 12.0, 13.6, 15.9, 17.9; (J+S)
B17	37	1	10	9, 6, 3	3, 3, 9, 3, 6, 6, 3, 3, 9, 3×3	2.2, 12.5, 15.7, 18.9, 22.2, 23.0, 23.3, 25.4, 33.7, 58.3, 61.9, 65.5
B18	37	2	10	9, 6, 3	9, 3, 6, 9, 9, 6, 3, 3	0.82, 1.7, 10.9, 12.5, 17.7, 21.4, 25.5, 28.5
B19	37	3	10	12, 9, 6	3, 3, 12, 6, 9, 6, 4×3	0.82, 10.7, 10.7, 10.7, 12.5, 14.0, 16.4, 16.4, 18.0, 20.0
B20	37	4	10	39, 15, 9	39, 9, 3×6	0.28, 10.7, 14.3, 18.1, 22.6

**Notes.** (J+S) – Jupiter and Saturn merged.

$f_I$ ), they are less stable, therefore they encounter each other and merge more easily; if the migration torques that they feel are weaker (i.e. large  $f_I$ ) they can more easily achieve a stable resonant configuration.

The embryos in sim. B8 move in low-eccentric orbits with semi-major axes from 9.9 to 21.7 AU, i.e. in a narrow range of heliocentric distance. Consequently, one may wonder whether the system would remain stable on a long time scale. In principle, a later instability may reduce the total number of embryos, in better agreement with our outer Solar System. To test this hypothesis, we extended all simulations listed in Table 2 up to 50 My. The final configurations at this time are summarized in PART B of this table. In general, the number of surviving embryos is reduced, as expected, but still too many embryos sur-

vive. Therefore, the formation and survival of too many planets seems to be a persisting problem. Notice that the embryos removed in late instabilities are not necessarily the least massive ones. For instance, in sim. B8, the most massive embryo is lost during a late instability and therefore also this simulation eventually does not satisfactorily reproduce the formation of Uranus and Neptune.

## 5. A “planet trap” at the edge of Saturn’s gap

In the previous section we have seen that a large fraction of the initial embryo population is lost due to migration into the Jupiter-Saturn region. Most of the embryos that come too close to the giant planets are eliminated because of collisions with

**Table 3.** Summary of the simulations accounting for a “planet Trap” at  $\sim 10$  AU.  $N$  is the initial number of embryos, each of  $3 M_{\oplus}$ .

No.	$N$	$f_d$	$m_{fin}$	$a_{fin}$
C1	10	3	12, 6, 3, 3	10.6, 9.8, 11.8, 12.9
C2	10	5	9, 6, 3, 3, 3	10.0, 11.1, 11.1, 11.1, 12.2
C3	10	10	12, 9, 6, 3	11.1, 9.9, 9.9, 9.9
C4	15	3	21, 3, 3	10.4, 11.5, 12.6
C5	15	5	18, 6, 3, 3, 3, 3	10.1, 12.1, 10.1, 11.7, 11.7, 12.7
C6	15	10	18, 9, 3, 3, 3, 3	10.2, 11.4, 11.4, 10.2, 10.2, 10.2

Jupiter and Saturn, ejection onto hyperbolic orbits or injection into the inner Solar System.

This result may be due to the fact that the migration torque that we implemented (from Cresswell & Nelson (2008) see Sect. 2), does not take into account the so-called coorbital corotation torque (Masset 2001). This torque would stop inward-migrating embryos at a “planet trap” just inwards of the outer edge of the gap opened in the disk of gas by Jupiter and Saturn (Masset et al., 2006). The planet trap would prevent the embryos from coming too close to the giant planets. To test which effects this would have on planetary accretion and evolution, we have done simulations implementing a new formula from Paardekooper et al. (2010), which accounts for the co-orbital corotation torque, as explained in Sect. 2.

We have first performed a series of three simulations. All started with a system of 10 embryos of  $3 M_{\oplus}$ , originally distributed from 11 to 34 AU, with a mutual orbital separation of 7 Hill radii. The simulations differed by the value of  $f_d$  we assumed: 3, 5 and 10. In all simulations  $f_I = 1$  because, in principle, there is no need to reduce Type-I migration speed as it automatically decreases to zero approaching  $\sim 10$  AU.

The results are summarized in the first three lines of Table 3, while an example of evolution is shown in Fig. 5, for the simulation with  $f_d = 10$ . After an initial phase of fast migration, all embryos come into the 10–12 AU region where, thanks to the strong eccentricity and inclination damping provided by the high disk surface density, they efficiently accrete with each other. Four planets are produced at the end. The most massive ones have 12 and  $9 M_{\oplus}$  and have distinct orbits, in resonance with each other. The two remaining bodies, of 6 and  $3 M_{\oplus}$  are all in the 1:1 MMR with the  $9 M_{\oplus}$  planet, forming a stable resonant configuration. No mass is lost in this run: the initial  $30 M_{\oplus}$  of material are all sequestered into the final four planets.

The runs with reduced gas density ( $f_d = 3, 5$ ) show a qualitative similar behavior. As there is less damping exerted onto the embryos, two embryos are lost in each of the simulations. In three out of four cases, an embryo was ejected beyond 1,000 AU. The remaining lost embryo was scattered into the inner Solar System. In these simulations, respectively 4 and 5 planets are produced in the end, the two most massive ones a bit smaller than in the  $f_d = 10$  case.

Overall, these experiments show that the planet trap is very effective in reducing the loss of mass during the embryo’s evolution. Still, the final results are not in good agreement with the structure of the Solar System. In fact, there are too many planets, protected from mutual collisions by resonances. Consequently, despite initially we have a total mass comparable to the combined mass of Uranus and Neptune, at the end the most massive

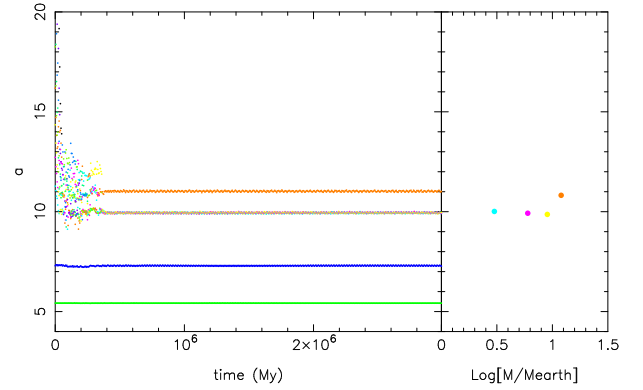


**Fig. 5.** The evolution of the semi major axes of the embryos in simulation C3. Each color represents a different embryo. The system stabilizes in  $\sim 200,000$  y. The panel on the right shows the final mass of the produced planets, as a function of their semi major axes. It highlights the existence of planets in co-orbital resonance with each other.

planets are not as big as the real planets because the total mass is distributed among 4 or 5 objects.

To test how these results would change with the total mass initially available in embryos, we ran a series of three additional simulations starting with 15 embryos of  $3 M_{\oplus}$ . The orbits of the embryos were initially separated by 5 mutual Hill radii and were distributed from 10 to 35 AU. Again, we assumed  $f_d = 3, 5$  and 10. The end-states are reported in the last three lines of Table 3. We find significantly more mass growth for the largest planet beyond Saturn which, in the end, achieves a mass of 18 or  $21 M_{\oplus}$ . However, the second planet does not grow nearly as much, never exceeding  $9 M_{\oplus}$ . Again, numerous embryos survive at the end of the simulations, protected from collisions in MMRs. Therefore, also this series of runs are not successful in reproducing the outer Solar System.

## 6. The initial mass of the embryos

All the simulations presented up to this point in the paper started from a system of embryos of individual mass equal to  $3 M_{\oplus}$ . In this section we study the influence of the individual mass of the embryos on the final results. Following the structure of the paper, we first present a series of simulations which do not account for the presence of a planet trap at the edge of Jupiter/Saturn’s gap, then we focus on the impact of the planet trap.

### 6.1. Without a planet trap

In this new series of simulations, we reduced the initial mass of embryos from 3 to  $1.5 M_{\oplus}$ . However, we increased the number of embryos from 14 to 23, thus basically preserving the total mass of the system. The embryos are initially located in the 10–35-AU interval with mutual orbital separations of 5 Hill radii.

The final states, at 8 My, of the simulations are summarized in Table 4. Although the number of merging events is slightly higher, as expected given that more bodies are in the system, the final masses of surviving embryos are, generally, lower than those with higher initial masses. In several cases, more mass is lost than in the runs starting with 14 embryos of  $3 M_{\oplus}$ . This is probably because the damping of eccentricity and inclination suffered from the disk is proportional to the individual mass of the embryo; therefore small embryos can more easily acquire



**Table 4.** Summary of simulations starting with 23 planetary embryos, each of  $1.5 M_{\oplus}$ . The final states are given at  $t = 8$  My. The effect of the planet trap is not taken into account.

No.	$f_d$	$f_l$	$m_{max}$	$m_{fin}$	$a_{fin}$
D1	1	1	3, 1.5, -	$7 \times 1.5$	11.4, 12.3, 17.8, 18.0, 27.9, 51.7, 68.0
D2	1	4	6, 4.5, 3	3, 4.5, 1.5, 3, 1.5	2.2, 9.6, 11.1, 11.2, 12.9
D3	1	10	4.5, 3, 1.5	1.5, 3, 1.5, 3, $5 \times 1.5$ , 4.5	2.5, 13.2, 14.6, 15.2, 15.4, 16.9, 18.6, 23.4, 27.8, 83.3
D4	2	1	3, 1.5, -	3, 1.5, 3, 1.5, 1.5	0.30, 9.9, 10.0, 12.1, 188
D5	2	4	7.5, 4.5, 3	7.5, 3, 1.5, 3	0.30, 9.6, 10.6, 19.8
D6	2	10	7.5, 6, 3	7.5, 1.5, 1.5	11.0, 14.0, 14.8
D7	3	1	1.5, -, -	$5 \times 1.5$	0.63, 9.5, 9.5, 9.5, 185
D8	3	4	7.5, 3, 1.5	1.5, 1.5, 7.5, 1.5	0.62, 8.9, 9.0, 10.5
D9	3	10	10.5, 7.5, 3	3, 10.5, 3	0.59, 15.6, 98.5
D10	4	1	9, 3, 1.5	$3 \times 1.5$	8.8, 8.9, 228
D11	4	4	6, 4.5, 1.5	6, 4.5, $3 \times 1.5$	0.33, 9.4, 10.7, 10.7, 11.5
D12	4	10	9, 4.5, 3	9, 3	10.9, 12.3

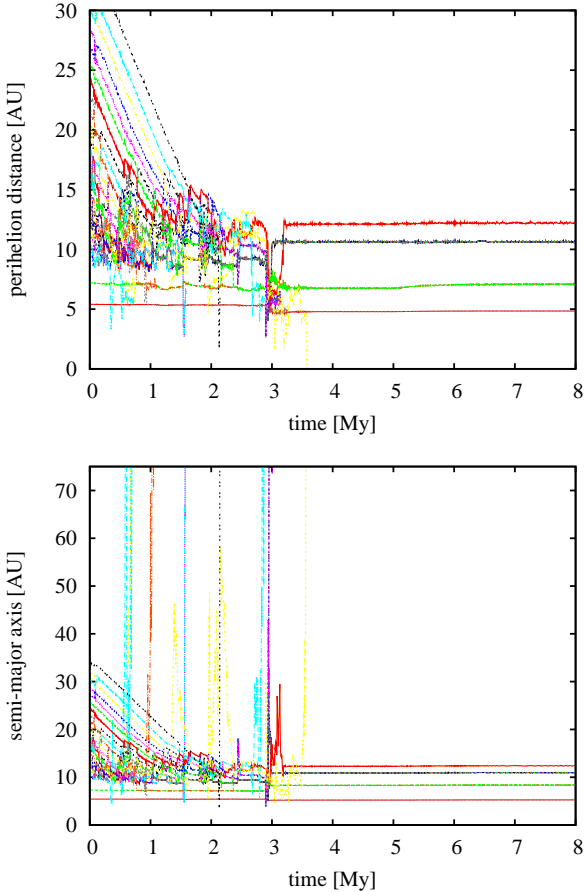


**Fig. 6.** The evolution of perihelion distance (upper plot) and semi-major axis (down plot) of bodies in simulation D12 (see Table 4).

**Table 5.** Like Table 3, but for the simulations starting from 36 embryos of  $1 M_{\oplus}$  each.

No.	$N$	$f_d$	$m_{fin}$	$a_{fin}$
E1	36	3	12, 2	10.3, 11.7
E2	36	5	14, 1, 1, 1, 1	10.3, 11.6, 11.6, 11.6, 12.9
E3	36	10	17, 4, 2, 1, 1	10.3, 11.3, 10.3, 10.3, 11.3

dynamically excited orbits that eventually intersect the orbits of the giant planets.

Only in two simulations, Nos. D9 and D12, an embryo with a mass equal or larger than  $9 M_{\oplus}$  is created and survives at 8 My beyond Saturn. Simulation D9 gives a picture unlike to our Solar System, since another two embryos, each with the mass of  $3 M_{\oplus}$ , are present at the end, the first is situated in the inner region and the second far beyond the present planetary region (semi-major axis equals  $\sim 100$  AU). In sim. D12 (Fig. 6), there are no redundant embryos. However, the masses of both surviving embryos are significantly lower than the mass of Uranus or Neptune; the mass of the first has risen to 9 and that of the second to only  $3 M_{\oplus}$ .

## 6.2. With a planet trap

We did a series of three simulations, starting from 36 embryos, each of  $1 M_{\oplus}$ . They are initially distributed from 9 to 35 AU, with a mutual orbital separation of 4.5 Hill radii. Like in Sect. 5 the values of the parameter  $f_d$  are 3, 5 and 10, whereas  $f_l = 1$  in all runs. Table 5 summarizes the final states of the systems.

The results are significantly different from those of the runs starting from more massive individual embryos. Only one planet is grown with masses of  $12 M_{\oplus}$  or more. However, the second most massive planet is very small. With the exception of simulation E1, more than 2 bodies survive at the end on stable, resonant orbits. More mass is lost in these simulations than in the corresponding simulations starting from more massive embryos. As said above, this is probably because the forces damping the eccentricities and inclinations of the embryos are weaker.

## 7. The effect of turbulence in the disk

The problems that we experienced in the previous sections due to embryos and proto-planets being protected by resonances from mutual collisions suggests that some level of turbulence in the disk might promote accretion. In fact, turbulence provides stochastic torques onto the bodies, inducing a random walk of their semi major axes (Nelson & Gressel 2010). If these torques are strong enough, the bodies may be dislodged from mutual resonances, which in turn would allow them to have mutual close encounters and collisions.

The problem is that it is not known a priori how strong turbulence should be in the region of the disk where giant planets form. The strength of turbulence depends on the level of ionization of the disk, and it is possible that in the massive regions of the disk where giant planets form the ionization of the gas is very low because the radiation from the star(s) cannot penetrate down to the midplane. Several formation models, therefore, argue that the planets form in a “dead zone” where, in absence of ionization, there is no turbulence driven by the magneto-rotational instability. This justifies the assumption that we made up to this point in the paper that the disk is laminar.

For sake of completeness, though, we test in this section how the results change if strong or weak turbulence is assumed in the

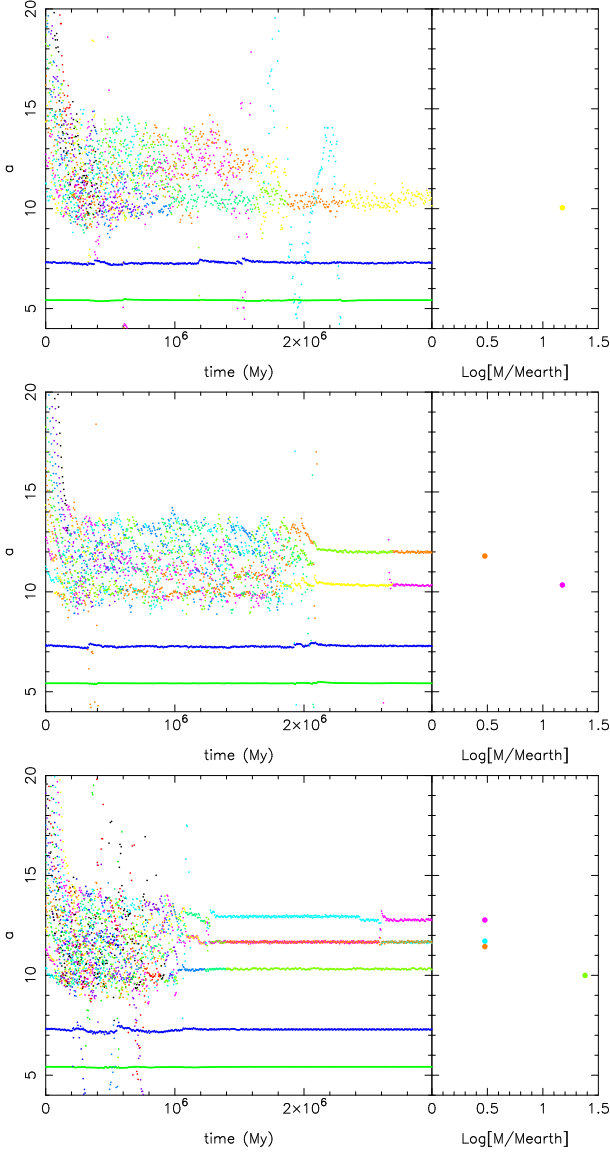


**Fig. 7.** The evolution of the semi major axes of the embryos in the simulations with  $f_d = 3$  and accounting for a planet trap and turbulence in the disk. The top panel is for a disk of embryos with a total mass  $M_T = 30 M_\oplus$  and  $\gamma = 3 \times 10^{-3}$ . The middle panel is for  $M_T = 30 M_\oplus$  and  $\gamma = 3 \times 10^{-4}$ . The bottom panel is for  $M_T = 45 M_\oplus$  and  $\gamma = 3 \times 10^{-4}$ .

disk. The experiments are conducted in the framework of the planet trap case with  $3 M_\oplus$  embryos (see Sect. 5), for a total of 30 and  $45 M_\oplus$  in disk of solids.

The top panel of Fig. 7 shows the result of a simulation with  $f_d = 3$ ,  $30 M_\oplus$  in the disk and  $\gamma = 3 \times 10^{-3}$ . This value to  $\gamma$  corresponds to strong turbulence with no dead zone. As one can see, in this case there is no permanent resonant trapping. A unique planet is formed with  $15 M_\oplus$ . Thus 50% of the mass is lost after close encounters with Jupiter or Saturn. Notice that, even when the surviving planet is alone in the system (i.e. after 2.4 My) its semi major axis is not steady, but has wide random fluctuation, as a result of the stochastic torques provided by the turbulence. A similar simulation, run with  $f_d = 5$ , gave no planets beyond Saturn in the end. This highlights the disruptive role of strong turbulence on planet formation.

The middle panel of Fig. 7 shows the evolution in a simulation with  $f_d = 3$  and  $30 M_\oplus$  in the disk, but  $\gamma$  decreased to  $3 \times 10^{-4}$ . Now turbulence is not strong enough to dislodge the last cores from the resonances. But it is strong enough not to allow 1/1 resonant objects and the survival of too many cores in general. So, the end-state is a system of only two planets beyond Saturn, which is a good result given the structure of the outer Solar System. However, only one of the two planets is massive enough ( $15 M_\oplus$ ) to reproduce Uranus or Neptune; the second one is a left-over embryo ( $3 M_\oplus$ ). This is because, again, almost 50% of the mass is lost despite of the planet trap mechanism.

Seeking for a more massive second planet, we ran a third simulation, with the same value of  $\gamma$ , but an initial embryo population for a total of  $45 M_\oplus$ . The result of this simulation is depicted in the bottom panel of Fig. 7. The mass of the most massive planet increases to  $24 M_\oplus$ . However, there is no significant growth for the second planet. Instead, three embryos with original masses survive at the end.

We conclude from these tests that weak turbulence may be helpful to break the isolation of planets and to avoid the formation of a too crowded planetary system beyond Jupiter and Saturn. However, the formation of two massive planets, with no left-over embryos seems to be still a distant goal.

## 8. Conclusions and Discussions

The formation of Uranus and Neptune by runaway/oligarchic growth from a disk of planetesimals is very difficult. The accretion rate is not large enough; moreover the accretion stalls when the major bodies achieve a few Earth masses (Safronov 1969; Levison & Stewart 2001; Levison & Morbidelli 2007).

In this paper, we have explored a mechanism for the formation of Uranus and Neptune that is different from those explored before. We assume that runaway/oligarchic growth from a planetesimal disk generated a system of embryos of 1–3 Earth masses, but not larger, in agreement with the results of Levison et al. (2010). Then, we follow the dynamical evolution of such a system of embryos, accounting for their mutual interactions, their interaction with a disk of gas and the presence of fully formed Jupiter and Saturn on resonant, non-migrating orbits. Because of computation speed, we do not perform the simulations with an hydro-dynamical code. Instead, we use a N-body code, and we apply fictitious forces to the embryos that mimic the orbital damping and migration torques that the disk exerts on the embryos. We use two prescriptions for the migration torque: one that ignores the co-orbital corotation torque and one that takes it into account. With the second prescription a “planet trap” (Masset et al. 2006) appears at about 10 AU, just inward of the outer edge of the gap opened by Jupiter and Saturn in the disk of gas.

Our results show that the idea works in principle. In many runs, particularly those accounting for a disk a few times more massive than the MMSN and in those accounting for the presence of the planet trap, there is a significant mass growth. In these cases, the major planet beyond Saturn exceeds 10 Earth masses. These results highlight the importance of the planet trap and of the damping effect that the gas-disk has on the orbital eccentricities and inclinations of planetary embryos.

None of our simulations, though, successfully reproduces the structure of the outer Solar System. Our results point to at least two major problems. The first is that there is typically a large difference in mass between the first and the second most massive planet, particularly in the simulations showing the most spectacular mass growth. This contrasts with Uranus and Neptune

having comparable masses. The second problem is that the final planetary system typically has many more than two planets, beside Jupiter and Saturn. Several original embryos, or partially grown planets, survive at the end on stable, resonant orbits. The simulations accounting for the planet trap are those that lead to the formation of the most complex, but stable planetary systems. In these systems, many bodies are in coorbital resonance with each other. This is in striking contrast with the outer Solar System, where there are no intermediate-mass planets accompanying Uranus and Neptune. It might be possible that these additional planets have been removed during a late dynamical instability of the planetary system, but the likelihood of this process remains to be proven.

Our simulations suggest that it is difficult to grow major planets without having a crowded planetary system at the end. In fact, the growth of a major planet from a system of embryos requires strong damping of eccentricities and inclinations from the disk of gas. But strong damping also favors embryos and planets to find a stable resonant configuration, so that systems with more surviving planets are found. Accounting for weak turbulence in the disk alleviates this problem. However, turbulence reduces the efficiency of the accretion process. If the mass of the disk is increased to compensate for this, we find again too many bodies surviving in the end beyond Saturn, with a too large mass ratio between the most massive one and the others.

In addition to the problems mentioned above, there is another intriguing aspect suggested by the results of our model. We have seen that, in order to have substantial accretion among the embryos, it is necessary that the parameter  $f_d$  is large, namely that the surface density of the gas is several times higher than that of the MMSN. However this contrasts with the common idea that Uranus and Neptune formed in a gas-starving disk, which is suggested by the small amount of hydrogen and helium contained in the atmospheres of these planets compared to those of Jupiter and Saturn. How to solve this conundrum is not clear to us.

In summary, our work does not bring solutions to the problem of the origin of Uranus and Neptune. However, it has the merit to point out non-trivial problems that cannot be ignored and have to be addressed in future work.

*Acknowledgements.* Part of this work was supported by France's EGIDE and the Slovak Research and Development Agency, grant ref. No. SK-FR-0004-09. RB thanks Germany's Helmholtz Alliance for funding through their 'Planetary Evolution and Life' programme.

## References

- Alexander, R. D., Clarke, C. J., & Pringle, J. E. 2006a, MNRAS, 369, 216  
 Alexander, R. D., Clarke, C. J., & Pringle, J. E. 2006b, MNRAS, 369, 229  
 Baruteau, C. & Masset, F. 2008, ApJ, 678, 483  
 Batygin, K. & Brown, M. E. 2010, ApJ, 716, 1323  
 Cresswell, P. & Nelson, R. P. 2008, A&A, 482, 677  
 Crida, A., Morbidelli, A., & Masset, F. 2007, A&A, 461, 1173  
 Duncan, M. J., Levison, H. F., & Lee, M. H. 1998, AJ, 116, 2067  
 Fernandez, J. A. & Ip, W.-H. 1984, Icarus, 58, 109  
 Goldreich, P., Lithwick, Y., & Sari, R. 2004a, ApJ, 614, 497  
 Goldreich, P., Lithwick, Y., & Sari, R. 2004b, ARA&A, 42, 549  
 Gomes, R., Levison, H. F., Tsiganis, K., & Morbidelli, A. 2005, Nature, 435, 466  
 Hahn, J. M. & Malhotra, R. 1999, AJ, 117, 3041  
 Hayashi, C. 1981, Progress of Theoretical Physics Supplement, 70, 35  
 Kley, W. & Crida, A. 2008, A&A, 487, L9  
 Levison, H. F. & Morbidelli, A. 2007, Icarus, 189, 196  
 Levison, H. F. & Stewart, G. R. 2001, Icarus, 153, 224  
 Levison, H. F., Thommes, E., & Duncan, M. J. 2010, AJ, 139, 1297  
 Lyra, W., Johansen, A., Zsom, A., Klahr, H., & Piskunov, N. 2009, A&A, 497, 869  
 Lyra, W., Paardekooper, S.-J., & Mac Low, M.-M. 2010, ApJ, 715, L68  
 Malhotra, R. 1993, Nature, 365, 819  
 Malhotra, R. 1995, AJ, 110, 420

- Masset, F. & Snellgrove, M. 2001, MNRAS, 320, L55  
 Masset, F. S. 2001, ApJ, 558, 453  
 Masset, F. S., Morbidelli, A., Crida, A., & Ferreira, J. 2006, ApJ, 642, 478  
 Morbidelli, A. & Crida, A. 2007, Icarus, 191, 158  
 Morbidelli, A., Crida, A., Masset, F., & Nelson, R. P. 2008, A&A, 478, 929  
 Morbidelli, A., Tsiganis, K., Crida, A., Levison, H. F., & Gomes, R. 2007, AJ, 134, 1790  
 Nelson, R. P. & Gressel, O. 2010, MNRAS, 409, 639  
 Ogihara, M., Ida, S., & Morbidelli, A. 2007, Icarus, 188, 522  
 Paardekooper, S.-J., Baruteau, C., Crida, A., & Kley, W. 2010, MNRAS, 401, 1950  
 Paardekooper, S.-J., Baruteau, C., & Kley, W. 2011, MNRAS, 410, 293  
 Paardekooper, S.-J. & Mellema, G. 2006, A&A, 459, L17  
 Paardekooper, S.-J. & Papaloizou, J. C. B. 2008, A&A, 485, 877  
 Pierens, A. & Nelson, R. P. 2008, A&A, 483, 633  
 Pollack, J. B., Hubickyj, O., Bodenheimer, P., et al. 1996, Icarus, 124, 62  
 Safronov, V. V. 1969, in Evolution of the Protoplanetary Cloud and Formation of the Earth and Planets (Nauka, Moscow)  
 Terquem, C. & Papaloizou, J. C. B. 2002, MNRAS, 332, L39  
 Thommes, E. W., Duncan, M. J., & Levison, H. F. 1999, Nature, 402, 635  
 Thommes, E. W., Duncan, M. J., & Levison, H. F. 2003, Icarus, 161, 431  
 Tsiganis, K., Gomes, R., Morbidelli, A., & Levison, H. F. 2005, Nature, 435, 459  
 Walsh, K. J., Morbidelli, A., Raymond, S., O'Brien, D. P. & Mandell, A. M. 2011, Nature, in press  
 Weidenschilling, S. J. 1977, Ap&SS, 51, 153